Two-Dimensional Electron-Positron Momentum Measurement at a Copper Single-Crystal Surface

R. H. Howell, P. Meyer, and I. J. Rosenberg
Lawrence Livermore National Laboratory, Livermore, California 94550

and

M. J. Fluss[a]
Argonne National Laboratory, Argonne, Illinois 60439
(Received 5 October 1984)

We report the first two-dimensional momentum measurements of annihilating positron-electron pairs at a solid surface. Positrons of 18 keV or 740 eV impinged on a clean Cu(121) surface. The 740-eV spectrum was resolved into two components, one associated with energetic positronium emission displaced from zero momentum and a second centered on zero momentum with distinct asymmetry for the directions parallel and perpendicular to the surface. The 18-keV spectrum was dominated by positron Bloch-state annihilation.

PACS numbers: 78.70.Bj, 61.55.Fe

In this Letter we report the first two-dimensional angular correlation (2D-ACAR) momentum-distribution measurements of annihilating positron-electron pairs employing monoenergetic positron beams. The combination of 2D ACAR with a variable-energy intense positron beam promises to reveal many features of both positron-surface physics and the properties of surfaces in general. New information about the condition of positrons bound at the surface and the production of positronium has been derived from these measurements. These first results were made at room temperature using an argon-sputter–cleaned ($<10\%$ surface contamination as measured by Auger analysis), annealed single crystal of Cu cut 2° from the [121] axis such that momentum distributions were obtained in the (111) plane where [101] was parallel to the surface and [121] was approximately perpendicular. The 2D ACAR surfaces reveal, by virtue of the forward momentum shift of the positronium (Ps) annihilation signal, the energetic Ps component which can be separated from the momentum distribution associated with surface and bulk states of the positron.

The low-energy positron beam is derived by moderation of high-energy positrons produced by pair production in a tungsten target irradiated by electrons at the Lawrence Livermore National Laboratory 100-MeV electron linac.[1] The high-energy positrons are moderated in tungsten vanes and a small fraction are emitted from the moderator surface as a result of the negative work function of the tungsten. These positrons are then electrostatically accelerated and transported along a magnetic guiding field to a UHV (2×10^{-10}-Torr) chamber located in a low-background area where the 8-mm-diam beam hits the sample. The linac was operated so that 3-μsec-wide positron pulses were produced at a rate of 900 s^{-1} for the 2D-ACAR measurements, and 15-nsec-wide pulses at a rate of 720 s^{-1} for the lifetime and time-of-flight (TOF) experiments.

The two-dimensional angular-correlation data were obtained using two position-sensitive Anger-camera gamma-ray detectors. Each Anger camera consists of a 400-mm-diam, 12.5-mm-thick NaI(Tl) plate with 37 75-mm-diam phototubes optically coupled to the plate. The usable field of view defined by a Pb collimator was 330 mm. The linear resolution was 8 mm, leading to an overall estimated angular resolution of 0.9 mrad at a distance of 13.67 m. The cameras are similar to those first used in 2D-ACAR studies of materials by West and co-workers[2]; however, several operational differences in the data acquisition and analysis were incorporated, as suggested by Smedskjaer and Fluss.[3] The high intensity of the positrons in the beam pulse (7×10^{9} s^{-1} instantaneous, 2×10^{7} s^{-1} time averaged) was limited by detector capabilities. Both the accidental backgrounds and the loss of events due to pileup rejection are greater than for similar experiments using continuous sources. For each beam pulse, pileup events were rejected by taking the first event in the energy window of each detector, while accidental coincidences were minimized by setting a narrow digital time window on the valid events. Events that satisfied all constraints, but were outside the time window, were also stored and processed into accidental 2D-ACAR spectra which were subtracted after normalization by multiplication of the accumulated accidental 2D-ACAR data by the ratio of in-window to out-of-window accidental counts in a time spectrum derived from the same data events as the ACAR.

Perspective drawings of the 2D-ACAR spectra obtained with the 18-keV and the 740-eV positrons are shown in Fig. 1. The data have been background subtracted and smoothed by the weighted average of three pixels along each axis. The positive p_z direction is along the positron beam direction into the surface. For 740 eV the sample was biased to attract re-emitted

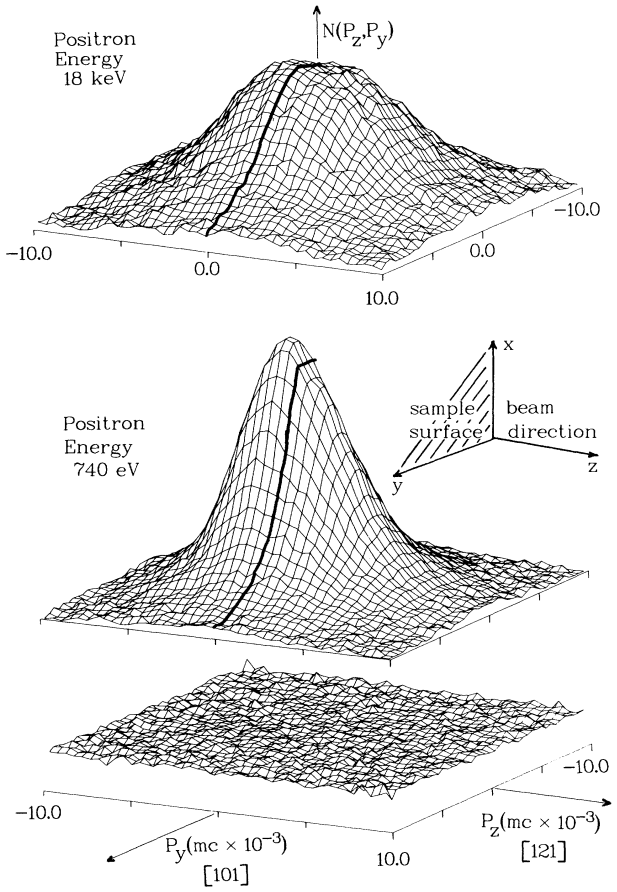

FIG. 1. The 2D-ACAR spectra for positron beams of 18 keV and 740 eV impinging on a single crystal of copper. The sample surface orientation and a typical background spectrum are also shown. The heavy contour at $p_z = 0$ emphasizes the asymmetry of the low-energy data.

positrons; for 18 keV it was set at zero to minimize surface positrons and enhance the bulk nature of the data. A typical accidental coincidence-background spectrum is shown with the 740-eV spectrum. Approximately 5×10^5 counts are shown in each of these spectra, representing ~ 24 h of data collection.

The data accumulated at 18 keV are similar to those reported by Berko and co-workers[4] for positrons annihilating in the bulk of an annealed Cu single crystal; the data are relatively flat from zero to 2.5 mrad, have a steeper slope from 2.5 to 5.5 mrad, and then are relatively flat again at the larger angles. In comparison, the 740-eV spectrum is much narrower overall, and highly asymmetric, with a narrow component riding on a broader base. This narrow component is shifted toward the negative p_z direction, as a result of the annihilation-in-flight of energetic Ps. Careful inspection of the 18-keV spectrum also reveals a small asymmetric Ps peak which masks the neck usually evident at zero momentum in this crystal orientation. The energetic Ps component was stripped from the underlying spectrum by subtraction of the spectrum for positive p_z from that for negative p_z. This procedure has the effect of clamping the asymmetric distribution to zero at zero momentum but only introduces significant error within 0.5 mrad of zero. The maximum energy of the positronium is equal to the value of the negative positronium work function. With the 0.9-mrad resolution taken into account, the maximum positronium momentum of $(4.5\pm0.25)\times10^{-3}mc$ was determined by integrating the positronium spectrum along the y direction and then extrapolating a straight line to zero positronium strength at the higher momenta. This corresponds to a work-function energy of -2.6 ± 0.15 eV in reasonable agreement with the value[5] of -2.4 eV obtained from electron and positron work-function values. The most probable Ps momentum is found at $p_z = 2.5\times10^{-3}mc$ and $p_y = 0.0mc$, corresponding to a forward energy of 0.80 eV. In an independent time-of-flight experiment[6] the maximum positronium energy was found to be 2.6 ± 0.3 eV, and the time distribution peaked at an energy of 1.1 ± 0.1 eV, in reasonable agreement with the present 2D-ACAR results. The yield of energetic Ps in the 740-eV spectra was 4% of the total counts for parapositronium implying 14% total Ps if a statistical distribution of spins is assumed.

The positronium momentum distribution can be calculated by use of conservation of energy and momentum if the electron-energy distribution and electron wave function in the metal are known.[7] If we assume that the positron momentum parallel to the surface plane is conserved, that the electrons are a free gas distributed evenly throughout the Fermi momentum sphere, and that the positronium-producing interaction is independent of the electron momentum, then the distribution of positronium in the momentum plane can be derived by conserving phase space between the material and the vacuum and integrating along the direction connecting the detectors. This results in

$$\frac{d^2N}{dK_z\,dK_y} = K_z 2^{-1/2}\sin^{-1}\left[\left(\frac{1-a_z^2-a_y^2}{2a_f^2-1+a_z^2-a_y^2}\right)^{1/2}\right],$$

where K_q is the momentum of the positronium and a_q is the positronium momentum divided by twice the square root of the product of the maximum positronium energy and the positron mass. The subscript q specifies either the y or z directions or the momentum value of the Fermi shell. The contours from this simple model are shown in the top of Fig. 2. The forward shapes of the contours in the data are qualitatively described by the model. However, significant deviations from the model contours occur for the position of the most probable momentum which is less in the data, $2.5\times10^{-3}mc$ (0.80-eV positronium energy), than in the model. These differences may be due to the known directional dependence of the Fermi surface at

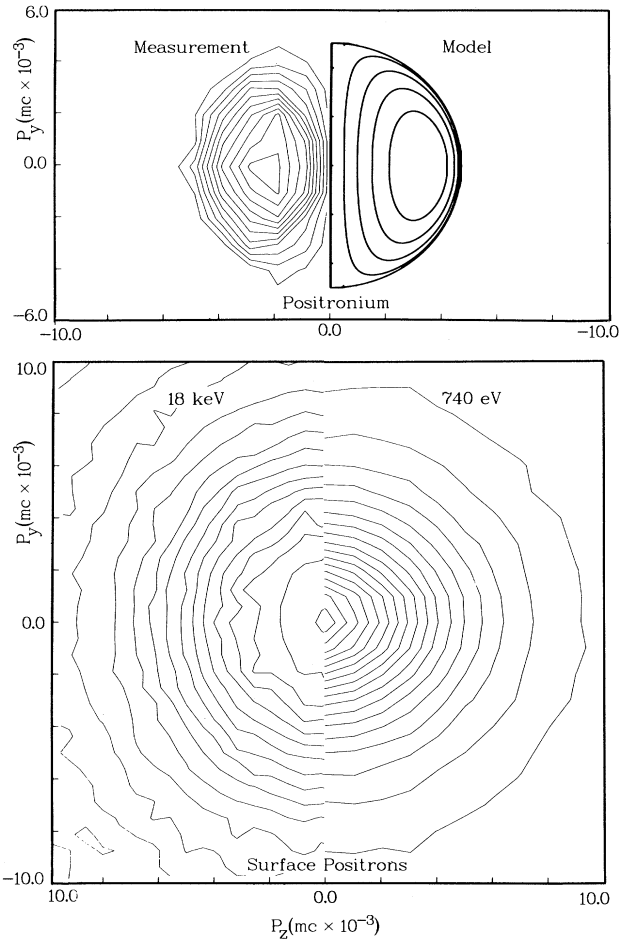

FIG. 2. Top, contour maps comparing measured and computed momentum distributions for positronium ejected from the copper surface. Bottom, positive-p_z contours for the 18-keV and 740-eV beams with no energetic positronium contribution.

the crystal-vacuum interface in copper. Also, if the positron-electron interaction depends on the electron momentum then distortions would be introduced into the momentum contours.

Because the positronium momentum is strongly shifted toward the vacuum, the differences between the high- and low-energy pair-momentum distributions for the opposite direction can be compared. At the bottom of Fig. 2 are contours of the spectra for the 18-keV and 740-eV beams for the momentum normal to the surface and directed into the sample. The flat background indicated in Fig. 1 was subtracted before plotting, the contour spacing was set at equal increments in each of the spectra, and the spacing level was chosen so that about the same number of contours appear in each spectrum. In the contour display of the data the narrowing of the pair-momentum distribution of positrons in the surface state compared to that distribution in the bulk can be seen to be the result of two phenomena: There is a loss of strength in the broad distribution of high-momentum components due to electrons bound at the ion core as evidenced by the very low number of lines for momenta greater than $6\times10^{-3}mc$ and there is also a narrowing of the peak in the low-momentum part of the distribution from the valence band. A similar narrowing of the angular correlation curve is seen in one-dimensional (1D) ACAR data for positrons trapped in vacancies and vacancy clusters where, again, the lower-momentum peak from valence electrons became sharper and the strength of the broad contribution from the core electrons was reduced.[8]

The width of the underlying momentum distribution from the 740-eV data is anisotropic with p_y narrower than p_z (6.6 ± 0.2 mrad vs 8.0 ± 0.2 mrad full width at half maximum). This is qualitatively different from trapping at vacancy clusters and voids which tends to produce isotropic distributions. The cutoff of the electron density perpendicular to the surface would be expected to lead to a momentum distribution for the valence electrons which is greater than that in the bulk. In the direction parallel to the surface, delocalization would lead to a narrowing of the momentum distribution. Such an asymmetry was predicted in the momentum distribution calculated with use of an independent particle model with a positron trapped in the surface-image–charge potential of aluminum.[9] There is also a strong inferred possibility that a localized or trapped Ps contribution may be contained in the broad part of the distribution. The present results account for a Ps yield of $\sim14\%$, while previous work[10] reports $\sim50\%$ Ps production from a clean Cu surface at room temperature. Lifetime measurements performed in the present experiments indicate significantly greater Ps yield than can be accounted for by the asymmetric part of the 2D-ACAR spectrum. We conclude that since no narrow Ps peak is seen, localized (and hence broadened) Ps must be contained in the underlying spectrum.

The authors wish to acknowledge stimulating discussions with Dr. J. Pendry, Dr. R. N. West, Dr. R. Prasad, Dr. R. Benedek, and also Dr. K. Lynn who showed us his preliminary data from a similar experiment in progress. The help of M. Connor and L. Bernardez in collecting the data, A. Coombs in developing the instrumentation, and J. Kimbrough in data acquisition software and hardware development is also gratefully acknowledged. This work was supported by the U. S. Department of Energy under Contracts No. W-7405-ENG-48 and No. W-31-109-ENG-38.

---

[a]Permanent address: Lawrence Livermore National Laboratory, Livermore, Cal. 94550.

[1]R. H. Howell, R. A. Alvarez, K. A. Woodle, S. Dhawan, P. O. Egan, V. W. Hughes, and M. W. Ritter, IEEE Trans. Nucl. Sci. **30**, 1438 (1983).

[2]R. N. West, J. Mayers, and P. A. Walters, J. Phys. E **14**, 478 (1981).

[3]L. C. Smedskjaer and M. J. Fluss, in *Nuclear Methods in Solid State,* edited by J. N. Mundy, S. J. Rothman, M. J. Fluss, and L.C. Smedskjaer, Methods of Experimental Physics, Vol. 21 (Academic, Orlando, Fla., 1983), p. 77.

[4]S. Berko, M. Haghgooie, and J. J. Mader, Phys. Lett. **63A**, 335 (1977).

[5]A. P. Mills, Jr., in *Positron Solid-State Physics,* edited by W. Brandt and A. Dupasquier (North-Holland, New York, 1983), p. 432.

[6]R. H. Howell, to be published.

[7]J. B. Pendry, in *Positron Solid-State Physics,* edited by W. Brandt and A. Dupasquier (North-Holland, New York, 1983), p. 408, and private communication.

[8]O. Sueoka, J. Phys. Soc. Jpn. **36**, 464 (1974).

[9]A. Alam, P. A. Walters, R. N. West, and J. D. McGervey, J. Phys. F **14**, 761 (1984); R. N. West, private communication.

[10]K. G. Lynn and D. O. Welch, Phys. Rev. B **22**, 99 (1980).